EFFECT OF MATRIX AND REINFORCEMENT POWDER TYPES ON TENSILE AND WEAR PROPERTIES OF TiB/Ti AND TiC/Ti COMPOSITES PREPARED BY SPS

Shoji Kamegawa[1], Hiroshi Izui[1], Yoshiki Komiya[1], Keisuke Kobayashi[1] and Ryohei Arimoto[1]

[1]Nihon University; 7-24-1, Narashinodai, Funabashi, Chiba, 274-8501, Japan

Keywords: Powder metallurgy, Spark plasma sintering, Titanium matrix composites

Abstract

Titanium and its alloys have low density, high specific strength, high fatigue strength, and good corrosion resistance. However, today they are underutilized in industry due to their high cost and poor wear resistance. To further improve their properties, TiB- and TiC-reinforced Ti matrix composites (TiB/Ti and TiC/Ti) were produced by the spark plasma sintering (SPS) process. The TiB and TiC distributions in the composites strongly affected their mechanical properties. We focused on how the matrix powder morphology and size affected their properties. Hydride-dehydride (HDH) and gas-atomized (GA) pure Ti powders with different powder sizes were used as a matrix, and TiB_2 or TiC powders were used as a reinforcement. We investigated the microstructures, the tensile properties, and the Vickers microhardnesses of the composites. The ultimate tensile strengths and the Vickers microhardnesses of the composites containing smaller HDH powders were higher than those containing GA powders.

Introduction

Titanium and its alloys have low density, high specific strength, high fatigue strength, good corrosion resistance, and good compatibility with carbon fiber reinforced plastic (CFRP) [1]. However, today they are underutilized in industry due to the high material cost and poor wear resistance. Adding ceramic particles into the metal matrix is one method of overcoming these drawbacks, leading to greater improvements in hardness, tensile properties, wear resistance etc. [2, 3]. Titanium-based ceramics such as TiB and TiC are stable in titanium, and their thermal expansion coefficients are close to that of titanium. TiB can be synthesized *in situ* as described by the following reaction formula (1) during the sintering process [4, 5]:

$$TiB_2 + Ti \rightarrow 2TiB \quad (1)$$

Powder metallurgy (PM) processes offer a promising cost-effective approach to the fabrication of titanium alloys in near-net-shape product forms. However, the conventional pressureless sintering of titanium alloys requires the use of a high sintering temperature (≥1,200 ºC) and a long isothermal hold time (≥120 min) for densification and microstructural homogenization. Even so, it is still difficult to achieve a pore-free homogeneous microstructure by pressureless sintering, particularly when high-strength titanium alloys that contain low-diffusivity elements are sintered [6]. In SPS, which is one type of PM process, uniaxial pressure and a pulsed direct current (DC) are applied to a graphite die and powder in a vacuum during sintering. This process can inhibit grain growth, allowing a high-density product to be obtained, due to sintering at a relatively low temperature and for a short time [6-8].

There have been many studies on the mechanical properties of titanium matrix composites. Titanium powders are roughly divided into two types: hydride-dehydride (HDH) and gas-atomized (GA) [9-11]. In previous studies, it has been found that sintered compacts containing smaller HDH powder (<45 μm) have higher ultimate tensile strengths than those containing GA powders [12]. However, there is not much data on how the tensile properties are affected by the matrix powder morphology and size and the type and amount of reinforcement. In this study, we used a smaller HDH powder (<20 μm) and focused on how the tensile and wear properties of TiB/Ti and TiC/Ti composites prepared by SPS were affected by the types of matrix and reinforcement powders.

Experimental procedure

Starting powders and SPS sintering process

We used three types of Ti powders as a matrix: HDH20 (nominal particle size <20 μm, average particle size 17.4 μm) and HDH45 (nominal particle size <45 μm, average particle size 27.3 μm, both from Toho Titanium Co., Ltd., Japan) prepared by the hydride-dehydride process, and GA45 (nominal particle size <45 μm, average particle size 20.2 μm, from Osaka Titanium Technologies Co., Ltd., Japan). We used two types of reinforcements: TiB_2 and TiC powders (particle sizes 1–2 μm, Japan New Metals Co., Ltd., Japan). Tables I and II show the chemical compositions of the starting powders. Figure 1 shows SEM micrographs of the powders, observed by a scanning electron microscope (SEM; SSX-550, Shimadzu Corporation, Japan).

Table I. Chemical compositions of titanium powders (wt%)

Element	Fe	Si	Mn	Mg	Cl	C	N	O	H	Ti
HDH20	0.03	0.01	<0.01	<0.001	0.001	<0.01	0.02	0.26	0.03	Bal.
HDH45	0.03	<0.01	<0.01	<0.001	0.001	<0.01	0.02	0.19	0.03	Bal.
GA45	0.038	-	-	-	-	0.005	0.009	0.106	0.004	Bal.

Table II. Chemical compositions of reinforcement powders (wt%)

Element	Total Carbon	Free Carbon	Fe	O	N	B	Ti
TiB_2	0.42	-	0.07	0.92	0.29	30.95	Bal.
TiC	19.73	0.20	0.15	0.57	-	-	Bal.

The powder mixtures were blended using a planetary ball mill (P-6, Fritsch Japan Co., Ltd., Japan) at a rotating speed of 200 rpm for 10 min in air. The mixed powders were filled into a graphite die (Toyo Tanso Co., Ltd., Japan), as shown in Figure 2(a), compressed to a pressure of 20 MPa by a hand press, and then sintered by SPS (DR.SINTER SPS-3.20MK IV, Sumitomo Coal Mining Co., Ltd., Japan) after being evacuated to below 10 Pa. Sintering was performed at a sintering temperature of 1173 K, a heating rate of 20 K/min, a sintering time of 10 min, and a pressure of 70 MPa, followed by furnace cooling.

Characterization tests

The composites prepared by SPS were polished with different emery papers up to #1200. Then, the relative densities of the composites were measured by Archimedes' method using an electric balance (BX-420H, Shimadzu Corporation, Japan). Vickers microhardness testing was carried out using a microhardness tester (HMV-2(T), Shimadzu Corporation, Japan). Tensile tests of the composites were performed at room temperature using an Instron-type machine (Instron,

MODEL 55R1125) at a cross-head speed of 0.5 mm/min. The microstructures and the fracture surfaces of the composites were characterized using SEM.

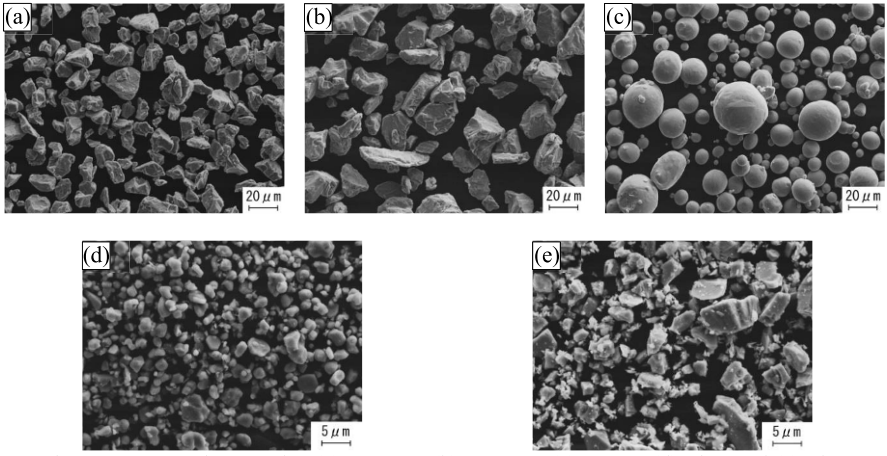

Figure 1. SEM micrographs: (a) HDH20, (b) HDH45, (c) GA45, (d) TiB_2 and (e) TiC.

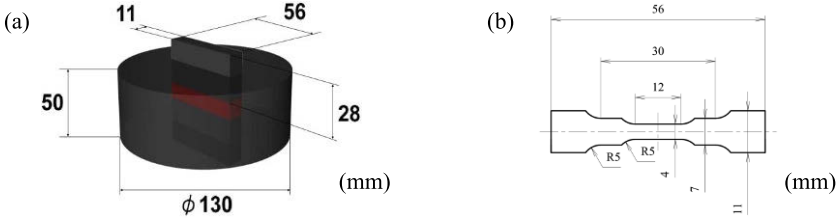

Figure 2. Schematic diagrams of graphite die and tensile test specimen.

In addition, wear tests will be carried out on a three-pin-on-disc wear test machine (MODEL EMF-3-F-ADX, A&D Company, Limited, Japan), using a vacuum heat-treated tool steel (SLD, Hitachi Metals, Ltd., Japan) for the pins and the prepared composites as discs. The disc to be used in the test has a square shape with dimensions 35 mm × 35 mm and 4 mm in thickness. The pin is 4 mm in diameter and 10 mm in height. Three pins are placed at 120 degree intervals on a circle with a diameter of 28 mm.

Results and discussion

Relative densities and microstructures of the composites

Figure 3 shows the relative densities of the composites. It is assumed that TiB_2 was perfectly transformed into TiB, and that TiC did not react with the Ti matrix during the sintering process. The relative densities of the composites were calculated using theoretical densities: Ti, 4.5 g/cc; TiB_2, 4.530 g/cc; TiB, 4.560 g/cc; and TiC, 4.920 g/cc [13, 14]. The relative densities of the TiB/Ti composites had nearly the same value of 99.5% up to 20 vol.% TiB. On the other hand, the relative densities of the TiC/Ti composites decreased with increasing TiC volume fraction.

Figure 4 shows the SEM micrographs of the composites. As shown in Figure 4 (a), TiB whiskers and clusters of them were observed between the matrix particles without the formation of pores. In the TiC/Ti composites, the pores between TiC particles increased in size with increasing TiC volume fraction. That is, the reduction in relative densities of the TiC/Ti composites is attributed to the presence of the pores.

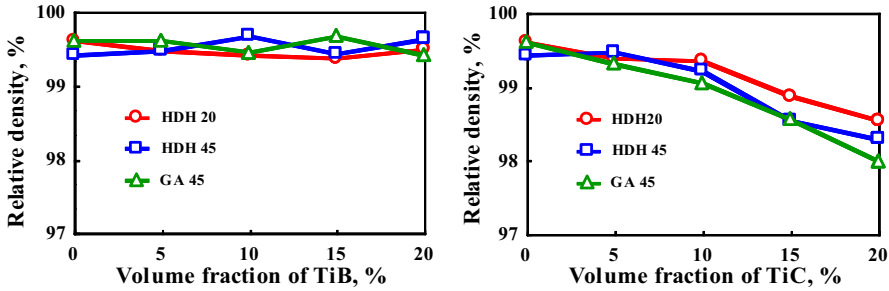

(a) TiB/Ti composites (b) TiC/Ti composites

Figure 3. Relationship between relative densities of the composites and reinforcement volume fraction.

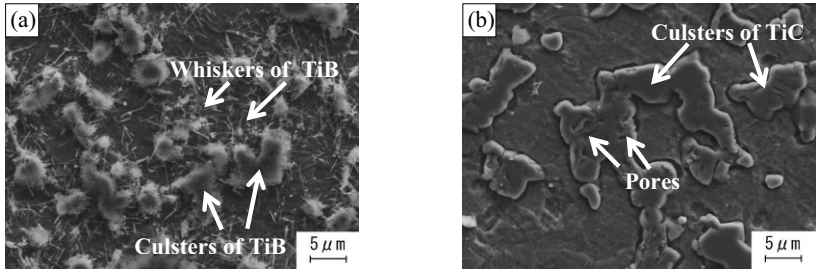

Figure 4. SEM micrographs of the composites with 15 vol.% reinforcement volume fraction: (a) 15TiB/Ti (HDH20) and (b)15TiC/Ti (HDH20).

Figure 5 shows the microstructures of the composites with a reinforcement volume fraction of 15 vol.%. Two phases can be observed in these micrographs, namely, TiB or TiC (black) and pure Ti (white). The reinforcements were evenly distributed in the HDH20 Ti matrix. However, for the HDH45 and GA45 composites, large agglomerations of the reinforcements were observed in the matrix.

Vickers microhardness and tensile properties of the composites

Figure 6 shows the effect of the reinforcement volume fraction on the Vickers microhardness of the composites. The microhardness increased in proportion to the increase of the reinforcement volume fraction. In particular, the addition of TiB to the Ti matrix led to a considerable hardness increase. These results suggest that TiB was more effective at increasing the microhardness than TiC was. Moreover, the microhardnesses of the composites containing HDH Ti particles were higher than those containing GA. The microhardnesses of the composites strongly depend on the oxygen content in the Ti matrix. The main reason for this is considered to be the solid solution

strengthening of oxygen into the titanium. The composites likely became harder and stronger due to oxygen dissolved in the titanium [15, 16], because the oxygen content of the GA was lower than that of HDH. This was due to the different oxygen contents due to differences in the manufacturing method and different specific surface areas of the Ti powders. GA powder is produced by using high-quality Ti stock (low-oxygen Ti feedstock) and a good protective atmosphere. Moreover, there is no contamination from the container during the GA manufacturing process [9-11].

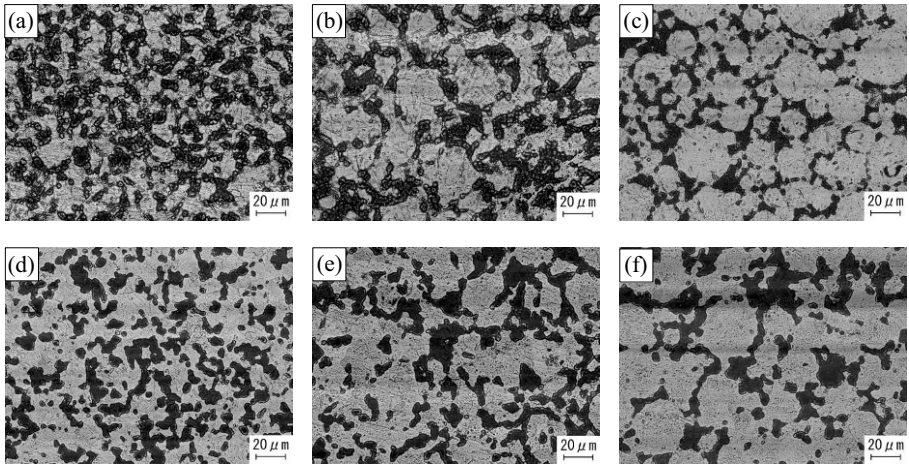

Figure 5. SEM micrographs of the composites containing different Ti powders: (a) 15TiB/Ti (HDH20), (b) 15TiB/Ti (HDH45), (c) 15TiB/Ti (GA45), (d) 15TiC/Ti (HDH20), (e) 15TiC/Ti (HDH45) and (f) 15TiC/Ti (GA45).

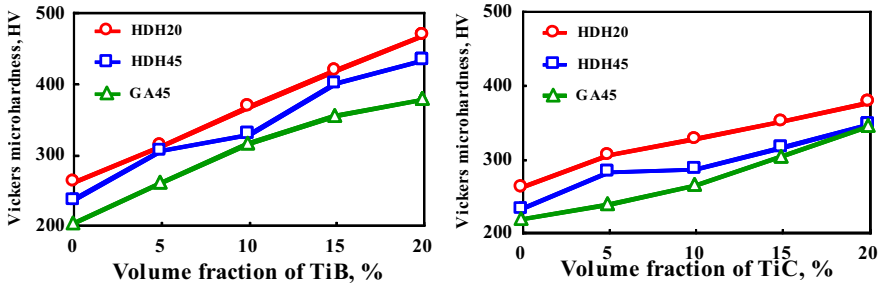

(a) TiB/Ti (b) TiC/Ti

Figure 6. Vickers microhardness versus reinforcement volume fraction of the composites.

The ultimate tensile strengths of the composites are shown in Figure 7. The composites with HDH20 had the highest ultimate tensile strengths. The maximum strengths of the composites with HDH and GA powders were obtained at reinforcement volume fractions of 15 vol.% and 20 vol.%, respectively. For the TiB/Ti composite with HDH20, the highest ultimate tensile strength was 1071 MPa at 15 vol.% TiB. Compared with the TiC reinforcement, the TiB/Ti composites had higher ultimate tensile strengths in all Ti matrix powders; however, the ultimate tensile

strengths of the TiC/Ti composites increased slightly as the TiC volume fraction increased. Therefore, the addition of TiB to the Ti matrix can lead to a considerable improvement in the ultimate tensile strength of the composites.

Figure 8 shows SEM micrographs of 15TiB/Ti (HDH20) and 20TiB/Ti (HDH20) composites. As shown in these figures, it is clear that the Ti matrix powders were surrounded by TiB clusters. In general, for particulate-reinforced composites, large agglomerations of the reinforcement particles act as stress concentrations in the matrix under tensile load. Therefore, many initial cracks are produced in the agglomerations, and these cracks are connected with each other. For a higher reinforcement volume fraction, a larger number of cracks are generated in the reinforcements [17, 18].

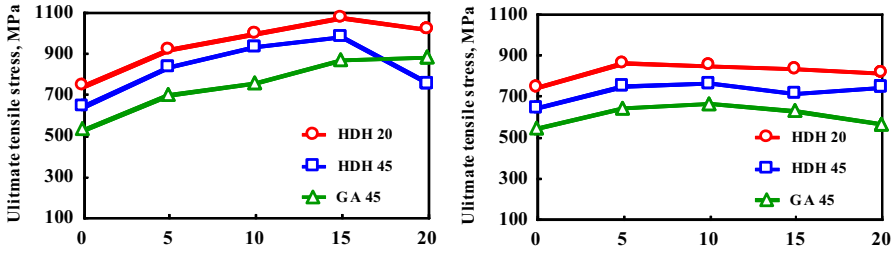

(a) TiB/Ti (b) TiC/Ti

Figure 7. Ultimate tensile stress versus reinforcement volume fraction of the composites.

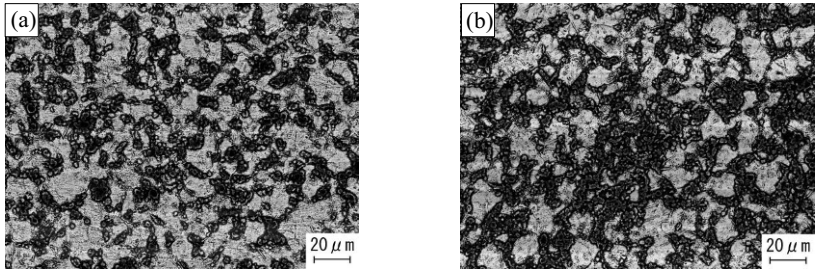

Figure 8. SEM micrographs of the composites: (a) 15TiB/Ti (HDH20), (b) 20TiB/Ti (HDH20).

Figure 9 shows the relationship between the reinforcement volume fraction and the elongation of the composites. All the elongations decreased with increasing volume fraction. The elongation of the TiC/Ti composites was higher than that of the TiB/Ti composites at volume fractions ranging from 10 to 20 vol.%. For the TiB/Ti composites, the ultimate tensile strength increased with increasing TiB volume fraction, as shown in Figure 7(a). Therefore, the elongation depended on the ultimate tensile strength. On the other hand, for TiC/Ti composites, the ultimate tensile strengths showed nearly the same values with an increase in the TiC volume fraction, as mentioned above.

As can be seen in Figure 4(b), there were a large number of pores in the TiC clusters. The fracture mechanism of the composite consists of particle fractures as a result of load transfer

from the matrix to the reinforcement followed by final failure via coalescence of micro-voids in the Ti matrix [18]. Therefore, in the TiC/Ti composites with the higher volume fraction, the increase in the number of the cracks in the TiC clusters let to the increase in the elongation of the composites.

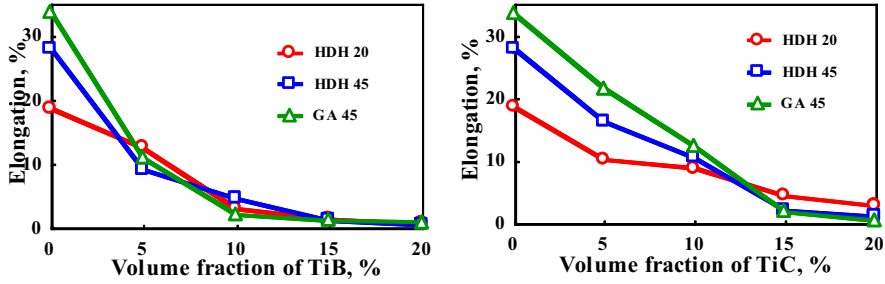

(a) TiB/Ti (b) TiC/Ti

Figure 9. Elongation versus reinforcement volume fraction of the composites

Conclusions

TiB/Ti and TiC/Ti titanium matrix composites were prepared by SPS. We investigated how the tensile properties of the composites were affected by the matrix powder morphology and size and the types and amounts of reinforcements. The following can be concluded.

(1) The relative density of TiB/Ti composites did not decrease by increasing the volume fraction of reinforcements but that of the TiC/Ti composites decreased.

(2) The TiB reinforcement was more effective at increasing the hardness and the ultimate tensile strength compared with TiC. The 15TiB/Ti (HDH20) composite showed the maximum ultimate tensile strength of 1071 MPa, and the 20TiB/Ti (HDH20) composite showed the maximum microhardness of 468HV.

References

1. Ikuhiro Inagawa et al., “Application and Features of Titanium for Aerospace Industry,” *Nippon Steel & Sumitomo Metal Technical Report*, 396 (2013), 23-28.

2. Takashi Saito and Tadahiko Furuta, “Development of High Performance Titanium Matrix Composite,” *R &D Review of Toyota CRDL*, 29 (3) (1994), 49-60.

3. Tadahiko Furuta et al., “Development of Titanium Metal Matrix Composite Exhaust Valve,” *R &D Review of Toyota CRDL*, 36 (1) (2001), 51-56.

4. K. B. Panda and K. S. Ravi Chandran, “Synthesis of Ductile Titanium–Titanium Boride (Ti-TiB) Composites with a Beta-Titanium Matrix: The Nature of TiB Formation and Composite Properties,” *Metallurgical and Materials Transactions A*, 34A (2003), 1371-1385.

5. N. S. Karthiselva et al., “Low Temperature Synthesis of Dense TiB_2 Compacts by Reaction Spark Plasma Sintering,” *International Journal of Refractory Metals & Hard Materials* (2015), 201-210.

6. Ya Feng Yang et al., “Composition of Spark Plasma Sintering of Elemental and Master Alloy Powder Mixes and Prealloyed Ti-6Al-4V Powder,” International Journal of Powder Metallurgy, 50 (1) (2014), 41-47.

7. Xiangbo Shen et al., “Microstructures and Mechanical Properties of the *in situ* TiB-Ti Metal-Matrix Composites Synthesized by Spark Plasma Sintering Process,” *Journal of Alloys and Compounds*, 509 (2011), 7692-7696.

8. Haibo Feng et al., “Spark Plasma Sintering Reaction Synthesized TiB Reinforced Titanium Matrix Composites,” *Composites: Part A*, 36 (2005), 558–563.

9. Kato Masamichi, “The Kind of Titanium Powder and its Applications, ” *Titanium.*, 57 (2) (2009), 130-133.

10. Fujita Makoto, “Manufacture of Titanium and Titanium-based Alloy Powders by Gas-Atomization, ” *Titanium.*, 54 (3) (2006), 196-198.

11. Harashima Kenji, “Manufacture of Titanium and Titanium-based Alloy Powders by HDH, ” *Titanium.*, 54 (3) (2006), 199-201.

12. Akinori Ota, *Effects of Raw Powder Morphology and Size on Tensile Properties of SPS-Consolidated TiB/Ti Composites* (Japan, Master's thesis of Nihon university, 2010).

13. E. A. Brandes, G. B. Brook, *Smithells Metals Reference Book Seventh Edition*, (Oxford, Butterworth-Heinemann Ltd, 1992), 14-2.

14. The Ceramic Society of Japan, *Handbook of Ceramic Engineerin*g (Japan, GihodoshuppanCo.,Ltd., 1989), 2026-2037.

15. Bin Sun et al., “Fabrication of high-strength Titan Ti Powder Materials by Oxygen Solid Solution Strengthening,” *Journal of Smart processing* , 1 (6) (2012), 283-287.

16. Mituo Niinomi, “Creation of Functionality by Ubiquitous Element in Titanium Alloys,” *Journal of the Japan Institute of Metals and Materials*, 75 (1) (2011), 21-28.

17. Hiroyasu Araki et al., “Mechanical Properties of Mechanically Alloyed TiC Particulate-Reinforced Titanium,” *Journal of the Japan Society of Powder and Powder Metallurgy*, 43 (10) (1996), 1247-1252.

18. S. C. Tjong and Yiu-Wing Mai, “Processing-Structure-Property Aspects of Particulate- and Whisker-Reinforced Titanium Matrix Composites,” *Composites Science and Technology*, 68 (2008), 583-601.

19. M. H. Loretto and D. G. Konitzerk, “The Effect of Matrix Reinforcement Reaction on Fracture in Ti-6Al-4V-Base Composite,” *Metallurgical Transactions A*, 21A (1990), 1579-1587.